Turkish Journal of Civil Engineering, 2026, xxxx-xxxx, Paper xxx, ***Research Article***

Evaluating the Effects of Two Modifiers on the Mechanical Properties of Sulfur Concrete Using a Novel, High-Capacity Lab-Scale Mixer for Sustainable Construction

Behnam RAFIE[1*]
Khaled MARAR[2]
Tulin AKCAOGLU[3]

ABSTRACT

Sulfur concrete represents a promising sustainable alternative to traditional Portland cement due to its rapid setting time, superior chemical resistance, and recyclability. Nonetheless, inherent brittleness and susceptibility to long-term deterioration limit broader applications, necessitating effective modifiers to improve mechanical and durability performance. This study investigates the influence of incorporating high density polyethylene (HDPE) and linear low-density polyethylene (LLDPE) at dosages of 5, 10, 15, and 20 wt.% into sulfur concrete containing 30 wt.% sulfur. Comprehensive evaluations included mechanical testing (compressive, flexural, and tensile strength), non-destructive testing methods (ultrasonic pulse velocity and rebound hammer), accelerated corrosion assessments via impressed voltage technique, and microstructural analyses (SEM, FTIR, and XRD). Results revealed optimum mechanical performance at 5 wt.% polymer content, with LLDPE modification achieving maximum compressive, flexural, and tensile strengths of 25.24 MPa, 3.31 MPa, and 1.75 MPa, respectively, compared to the control's 20.6 MPa, 2.75 MPa, and 1.21 MPa. Corrosion resistance significantly improved with polymer additions, notably at 20 wt.% LLDPE exhibiting the lowest current intensity (~0.03 A). SEM analysis confirmed enhanced matrix density with HDPE modification, whereas FTIR and XRD analyses indicated no

Note:
- This paper was received on August 15, 2025 and accepted for publication by the Editorial Board on January 9, 2026.
- Discussions on this paper will be accepted by xxxxxxx xx, xxxx.

• https://doi.org/

1 Eastern Mediterranean University, Department of Civil Engineering, Famagusta, Turkish Republic of Northern Cyprus
behnam.rafie@emu.edu.tr - https://orcid.org/0000-0001-9347-1335

2 Eastern Mediterranean University, Department of Civil Engineering, Famagusta, Turkish Republic of Northern Cyprus
khaled.marar@emu.edu.tr - https://orcid.org/0000-0001-5650-2980

3 Eastern Mediterranean University, Department of Civil Engineering, Famagusta, Turkish Republic of Northern Cyprus
tulin.akcaoglu@emu.edu.tr - https://orcid.org/0000-0002-9597-4320

* Corresponding author

chemical interactions, affirming physical blending. These findings highlight that carefully selected polymer modifications significantly enhance the mechanical integrity and durability of sulfur concrete for sustainable infrastructure applications.

Keywords: Sulfur concrete, lab-scale production, sulfur concrete mixer, polymer modifier, compressive strength.

1. INTRODUCTION

Concrete remains the most widely used construction material globally, primarily owing to its versatility, durability, and cost-effectiveness. However, the extensive use of traditional Portland cement concrete (PCC) has severe environmental implications, particularly due to high CO_2 emissions during cement manufacturing, accounting for approximately 7% of global anthropogenic CO_2 emissions [1]. Consequently, developing sustainable alternative materials with lower ecological impacts is imperative for the future of construction. Among these alternatives, sulfur concrete (SC) has emerged as a promising candidate due to its advantageous properties such as superior resistance to corrosive and acidic environments, absence of hydration water dependency, and availability of sulfur as an abundant and inexpensive byproduct from petroleum refining processes [2–5].

Research into sulfur concrete has expanded significantly, highlighting its potential for specialized construction applications, including chemical-resistant structures, waste storage facilities, and extraterrestrial construction scenarios such as lunar and Martian habitats [6–8] Additionally, sulfur concrete's rapid solidification and ability to achieve high early strength without water usage provide significant logistical advantages in arid regions and remote construction sites [9]. However, despite these notable advantages, sulfur concrete's widespread adoption has been hindered by critical limitations, particularly related to its brittleness, long-term structural instability, and susceptibility to thermal degradation and cracking over extended periods [8,10,11]

To address these limitations, various modification techniques have been explored. Modifiers such as dicyclopentadiene (DCPD), cyclopentadiene, dipentene, olefin polysulfide additives, bitumen, and melamine have shown promising results in enhancing the mechanical and durability properties of sulfur concrete [6,12–14]. For instance, incorporating modifiers like DCPD has demonstrated improvements in mechanical strength; however, the practical application is complicated by the exothermic and unstable nature of sulfur-DCPD reactions [7,15,16] . Recent research has shifted towards polymeric modifiers such as high-density polyethylene (HDPE) and linear low-density polyethylene (LLDPE), owing to their potential to significantly enhance the ductility and mechanical performance of sulfur concrete through physical reinforcement mechanisms, without adverse chemical interactions [17–20].

Although considerable research attention has been devoted to modifying sulfur concrete, the existing literature also highlights a critical gap related to the production methods used for preparing laboratory-scale specimens. The inadequacy of current mixing equipment in terms of capacity, temperature uniformity, and consistent material dispersion has led to issues regarding the reproducibility and reliability of experimental outcomes. Existing laboratory mixers generally produce insufficient specimen quantities and exhibit uneven temperature

distribution, necessitating multiple mixing cycles and prolonged processing times, thereby increasing research costs and complexity [10,14,21].

To bridge this identified gap, the present study introduces a novel, high-capacity, temperature-controlled laboratory-scale mixer specifically designed to produce consistent, high-quality sulfur concrete specimens in a single mixing operation. This research also systematically evaluates the mechanical, microstructural, and durability properties of sulfur concrete modified with HDPE and LLDPE at different concentrations (5, 10, 15, and 20 wt.-%). By integrating comprehensive mechanical testing and microstructural characterization methods, this study aims to identify the optimal modifier concentration that achieves the best balance of mechanical performance, stability, and durability. Thus, the outcomes of this research provide critical insights and practical solutions to overcome the existing limitations in sulfur concrete production and modification, promoting its broader application as a sustainable construction material.

2. MATERIALS AND METHODS

2.1. Materials

Fig.1 shows all the materials used in this study, which were carefully selected to maintain high-quality standards and achieve optimal results in terms of mechanical properties and durability of the modified sulfur concrete. The elemental sulfur used in this study , had a

Fig.1 - Materials used: elemental sulfur, heating oil, aggregates, LLDPE, and HDPE polymers.

purity level of 99%. Two types of polymer modifiers were utilized: high density polyethylene (HDPE) with a density of 940 kg.m^{-3}, and linear low-density polyethylene (LLDPE) with a density of 920 kg.m^{-3}. Both polymer modifiers were and were used as received without additional processing. The heating medium employed was Diala S4 (ZX-I), a medium-viscosity oil produced by Shell, specifically selected due to its high flash point of 191 °C, which ensures safe and stable thermal conditions during the sulfur concrete mixing process.

Aggregates for concrete preparation were sourced locally from a concrete batching plant in Cyprus, consisting of natural fine and coarse aggregates. A detailed sieve analysis was conducted following ASTM C33 standard [22] to determine particle size distribution and ensure compatibility with sulfur concrete formulations, Fig.2. The fine aggregate primarily consisted of particles smaller than 0.6 mm, contributing to the overall homogeneity of the sulfur concrete by acting as fillers, while coarse aggregates met standard gradation limits to enhance the mechanical properties. The fine and coarse aggregates also satisfied the physical requirements of ASTM C33, with oven-dry specific gravity of about 2.6, water absorption below 2%, and moisture content during batching kept below 1%.

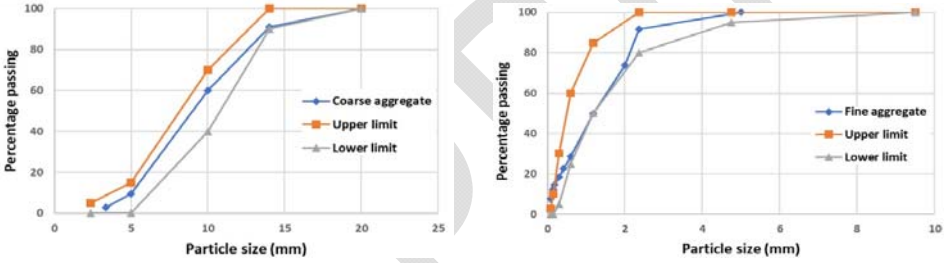

(a) (b)

Fig.2 - Grading curves of (a) Coarse aggregate and (b) fine aggregate

2.2. Design and Production of a Temperature-Controlled Laboratory Mixer

This study aimed to develop a reliable and efficient laboratory-scale mixing device specifically designed for preparing sulfur concrete. The key objectives included ensuring uniform heat distribution, precise temperature control, and sufficient mixing capacity to produce homogeneous sulfur concrete specimens. The designed mixer comprises two separate reservoirs: an outer reservoir containing heating oil to ensure uniform temperature distribution, and an inner reservoir dedicated to mixing sulfur concrete materials (Fig.3).

The inner reservoir has a capacity of approximately 0.091 m^3, which is sufficient for casting ten prism specimens measuring 100 × 100 × 500 mm each. Uniform heat distribution is achieved through an oil bath method, utilizing Diala S4 (ZX-I) oil, heated via two 3 kW electrical elements. The dual heating elements offer several advantages, including the ability to operate at half or full capacity to optimize energy use and provide redundancy in case of element failure, thereby ensuring continuous operation. Additionally, the outer layer of the mixer is insulated using glass wool to minimize heat losses and maintain thermal efficiency.

The mixer is equipped with a heavy-duty mortar mixer integrated into an insulated removable cover, providing adjustable mixing speeds ranging from 180 to 460 rpm. This cover minimizes heat transfer and prevents energy wastage during operation. A dedicated control unit is incorporated to precisely manage the heating process, maintaining a stable temperature of up to 180 °C, and preventing thermal overshoot or runaway during extended mixing durations of approximately four hours. These design features provide stable thermal conditions and allow continuous mixing of relatively large batches, which is beneficial for achieving reliable and reproducible sulfur concrete production at the laboratory scale.

Fig.3 - Custom-built temperature-controlled mixer for sulfur concrete: external view, mixing chamber, control panel, and heating system layout.

2.3. Mix Design of Modified Sulfur Concrete

An effective mix design is essential for achieving optimal properties in sulfur concrete. The proportion of elemental sulfur significantly influences the mechanical and durability characteristics of sulfur concrete. Based on existing literature and established best practices, a sulfur content of approximately 30 wt.% of the total concrete mixture (by mass) was selected due to its optimal balance between mechanical strength, durability, and ease of workability [23,24]. Lower sulfur content typically results in inadequate binding, while excessively high sulfur content can lead to brittleness and thermal instability.

Modifiers such as HDPE and LLDPE were introduced at concentrations of 5, 10, 15, and 20 wt.-% by mass of elemental sulfur, based on previously reported optimal ranges for polymer modified sulfur concretes. Existing studies suggest that polymer additions ranging from approximately 5 wt.% to 20 wt.%. significantly influence the mechanical and durability properties of sulfur-based composites, enhancing ductility, toughness, and resistance to

cracking [23,25]. The selection of this range enabled a comprehensive evaluation of mechanical performance and the identification of the optimal modifier concentration.

A mixture of 26 wt.-% coarse aggregate and 44 wt.-% fine aggregate , expressed as mass fractions of the total sulfur concrete mixture (sulfur plus aggregates), was identified through preliminary trials to produce a homogenous concrete without the need for compaction, aligned with established practices in producing self-compacting concretes [26]. Table 1 presents the final mixture proportions for the control and modified sulfur concrete specimens, ensuring that the total summation reaches 100 wt.-% for accurate representation and reproducibility.

Table 1 - Mixture proportions of control and polymer-modified sulfur concretes.

specimen Name	sulfur (wt.-%)	coarse (wt.-%)	sand (wt.-%)	HDPE (wt.-%)	LLDPE (wt.-%)
Control	30	26	44	0	0
5 HDPE	30	26	44	5	0
10 HDPE	30	26	44	10	0
15 HDPE	30	26	44	15	0
20 HDPE	30	26	44	20	0
5 LLDPE	30	26	44	0	5
10 LLDPE	30	26	44	0	10
15 LLDPE	30	26	44	0	15
20 LLDPE	30	26	44	0	20

Table 2 - Absolute mixture proportions

Specimen	Sulfur (kg/m^3)	Coarse aggregate (kg/m^3)	Sand (kg/m^3)	HDPE (kg/m^3)	LLDPE (kg/m^3)	Unit weight (kg/m^3)
Control	720	624	1056	0	0	2400
5 HDPE	720	624	1056	36	0	2436
10 HDPE	720	624	1056	72	0	2472
15 HDPE	720	624	1056	108	0	2508
20 HDPE	720	624	1056	144	0	2544
5 LLDPE	720	624	1056	0	36	2436
10 LLDPE	720	624	1056	0	72	2472
15 LLDPE	720	624	1056	0	108	2508
20 LLDPE	720	624	1056	0	144	2544

In addition, Table 2 presents the absolute mixture proportions, normalized to 1 m^3 of concrete (kg/m^3), together with the corresponding unit weight of each mixture, calculated from the relative mass fractions reported in Table 1 and the unit weight of the control sulfur concrete.

2.4. Sulfur Concrete Specimen Preparation

Sulfur concrete specimens were prepared using the laboratory-scale mixer designed in this study, as described in Section 2.2. Initially, elemental sulfur was introduced into the mixing reservoir once the temperature of the heating oil bath reached approximately 150 °C. Upon melting, which was visually confirmed by the transition of sulfur color to light orange, polymer modifiers (HDPE or LLDPE) were incrementally added to the molten sulfur every 10 minutes to ensure uniform dispersion within the sulfur matrix. This polymer-sulfur mixture was continuously mixed for a total duration of four hours to achieve optimal homogeneity.

Following the preparation of the homogeneous sulfur-polymer blend, preheated coarse and fine aggregates (heated to 180 °C in a convection oven to minimize thermal shock and enhance compatibility) were gradually incorporated into the mixture. The complete mixing process, inclusive of aggregate addition, required approximately four and a half hours from the point of sulfur melting.

The final concrete mixtures were then poured directly into unheated molds without additional compaction or vibration, leveraging the self-compacting nature of the mixture. Cylindrical (100 mm diameter × 200 mm height) and prism (100 × 100 × 500 mm) molds were used to produce specimens suitable for various mechanical property evaluations (Fig. 4). The specimens were demolded after solidification and allowed to cure under laboratory conditions for three days prior to testing. Fig.4 illustrates freshly cast sulfur concrete in a cylindrical mold and hardened specimens in prism and cylindrical shapes, demonstrating the final appearance and structural integrity of the prepared samples.

Fig.4 - Fresh and hardened sulfur concrete specimens in cylindrical and prism molds.

2.5. Experimental Methods

2.5.1. Compressive, Tensile, and flexural strength tests

To comprehensively evaluate the mechanical properties of the modified sulfur concrete, standardized tests for compressive, tensile, and flexural strength were conducted, following international testing procedures. The compressive strength of sulfur concrete specimens was assessed using cylindrical samples measuring 150 mm, tested according to BS EN 12390-3 [27]. This test provides crucial insights into the ability of sulfur concrete to withstand loads commonly encountered in structural applications such as industrial flooring, sewer pipes, and pavement structures.

The splitting tensile strength, an essential indicator of the resistance of sulfur concrete to tensile stresses and cracking, was determined using cubic specimens in accordance with BS EN 12390-6 [28]. Tensile strength assessment is vital for predicting the performance of sulfur concrete in applications susceptible to tensile stresses, such as bridge decks, pavements, and other load-bearing structures.

Fig.5 - Experimental setup for evaluating mechanical properties: tensile, compressive, and flexural strength testing

Flexural strength was measured using prism specimens (100 × 100 × 500 mm), subjected to third-point loading in accordance with ASTM C78 standard [29]). Flexural strength testing is particularly significant for sulfur concrete applications involving bending loads, such as pavement slabs and structural beams. Fig.5 illustrates the standardized test setups employed for evaluating compressive, tensile, and flexural strengths, demonstrating the configurations and apparatus used in each respective mechanical test.

2.5.2. Ultrasonic Pulse Velocity and Schmidt Hammer Tests

Non-destructive testing (NDT) methods were employed to evaluate the in-situ quality and compressive strength of concrete specimens. Initially, rebound values were recorded using a SilverSchmidt hammer (N-Type, standard energy of 2.207 Nm) according to EN 12504-2 [30] and ASTM C805 standards [31]. Prior to testing, the concrete surface was smoothed with a grinding stone, and at least nine impacts were performed per sample. The test was conducted perpendicular to the surface, with impact points spaced a minimum of 25 mm apart. Median values were calculated to assess uniformity and serve as input for strength estimation.

Subsequently, Ultrasonic Pulse Velocity (UPV) testing was conducted using the Pundit Lab+ system to determine pulse velocity and transmission time (μs) through direct transmission across the specimen [32]. The testing parameters were set with an excitation voltage of 500 V and a receiver gain of 200×(signal amplification factor), ensuring optimal signal clarity. Each sample was tested using standard 54 kHz transducers, and transmission times were averaged for accuracy. Fig.6 illustrates the experimental setup for Schmidt hammer and UPV testing.

Fig. 6 - Setup for UPV and Schmidt hammer tests on sulfur concrete specimens.

For strength estimation, the SONREB method [32] was employed, which integrates rebound values, R (from the SilverSchmidt), and UPV results, $\boldsymbol{v}$. The Pundit Lab+ was configured with a pre-defined conversion curve based on the function [33]

$$(v, R) = a \cdot v^{b} \cdot R^{c} \quad (1)$$

$where\ a = 8.31 \times 10^{-11}$, $b = 2.81$, $and\ c = 0.86$; v is the ultrasonic pulse velocity (m/s), R is the rebound number (dimensionless), and $f(v, R)$ is the estimated compressive strength (MPa).

This enabled computation of compressive strength directly from measured rebound and pulse velocity data. As illustrated in Fig. 7, the predefined SONREB conversion curve used in the Pundit Lab+ system visualizes the correlation between the rebound number, pulse velocity, and the estimated compressive strength.

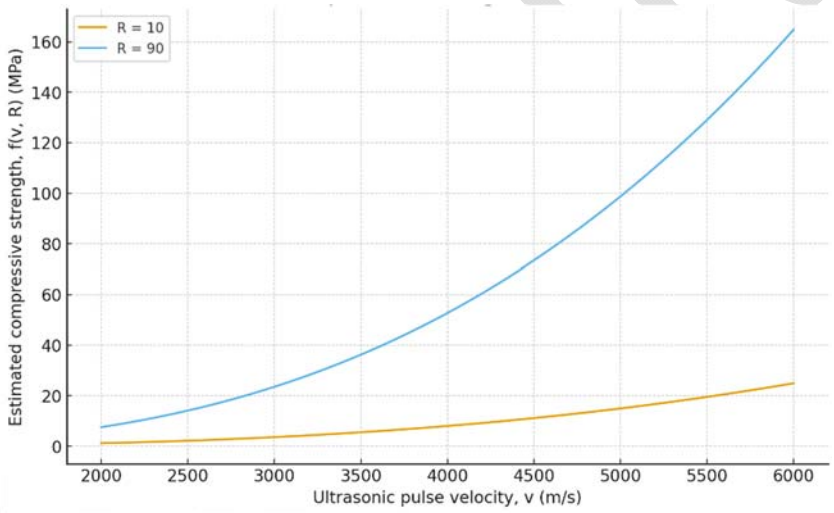

Fig.7 - Conversion curve for compressive strength estimation using the SONREB method in Pundit Lab+.

2.5.3. Microstructural Analysis

Microscope Examination: The surface morphology of modified sulfur concrete specimens was initially examined using an optical stereomicroscope (Euromex), providing preliminary visual insights into the microstructure at low magnifications. This microscopic technique enables the direct observation and measurement of surface features, such as aggregate distribution, voids, and potential defects, within the specimen matrix. Digital imaging software facilitated precise dimensional measurements of specific structural elements, contributing to a detailed morphological characterization of the concrete specimens. For stereomicroscope observations, small fragments were cut from the mid-depth of the prisms

after mechanical testing. The exposed surfaces were gently ground and cleaned to remove loose particles and obtain a flat surface suitable for low-magnification imaging.

Scanning Electron Microscopy (SEM): Scanning Electron Microscopy (SEM) analyses were performed using a JEOL JSM-6610LV microscope to study the detailed microstructural features of sulfur concrete at high magnifications. Specimen surfaces were prepared through careful fracture to reveal internal structures. SEM analysis operates by scanning the surface with a focused electron beam, generating secondary electrons that produce high-resolution images. Microstructural features, including matrix homogeneity, aggregate-binder interfaces, polymer dispersion, and pore structure, were systematically evaluated, providing valuable insights into the effects of polymer modifiers on the microstructure of sulfur concrete. For this test, representative pieces were taken from the fractured surfaces, oven-dried at 40–50 °C, mounted on aluminium stubs with carbon tape, and sputter-coated with a thin gold layer to ensure sufficient electrical conductivity during imaging.

Fourier-Transform Infrared Spectroscopy (FTIR): FTIR spectroscopy was conducted to identify chemical bonds and evaluate potential interactions between sulfur and polymer modifiers. FTIR spectra were obtained using an attenuated total reflectance (ATR) mode, scanning samples over a wavenumber range of 400–1600 cm^{-1}. The FTIR technique identifies molecular vibrations by measuring the absorption of infrared radiation by chemical bonds within the material. The characteristic absorption peaks detected provided critical information regarding the stability and chemical compatibility of sulfur and polymers, verifying whether any chemical reaction or significant molecular-level interaction occurred during mixing and curing. FTIR samples were prepared by scraping a thin layer of material from the sulfur matrix; the resulting powder was gently pressed onto the ATR crystal to achieve good contact before recording the spectra.

X-Ray Diffraction (XRD): X-Ray Diffraction (XRD) analyses were carried out using a diffractometer operating with Cu-Kα radiation at a wavelength λ = 1.5406 Å to investigate the crystalline phase composition of sulfur concrete specimens. Powdered samples extracted from crushed sulfur concrete were scanned within a 2θ range of 10°–70° at a scanning rate of 2°/min. The recorded diffraction patterns were interpreted according to Bragg's law:

$$n\lambda = 2d \sin \theta \quad (2)$$

Where n is an integer representing the order of diffraction, λ is the X-ray wavelength, is the distance between atomic lattice planes, and θ is the diffraction angle. The analysis provided crucial information about the phase composition and crystallinity, enabling the assessment of potential changes in crystal structure resulting from polymer modification in sulfur concrete.

For XRD analysis, selected fragments were crushed in an agate mortar and sieved to obtain a fine powder (particle size below about 75 μm), which was then placed in the sample holder and levelled to provide a smooth, uniform surface for diffraction measurements.

Fig.8 presents the equipment used for microstructural analysis, including optical microscopy, SEM, FTIR, and XRD techniques.

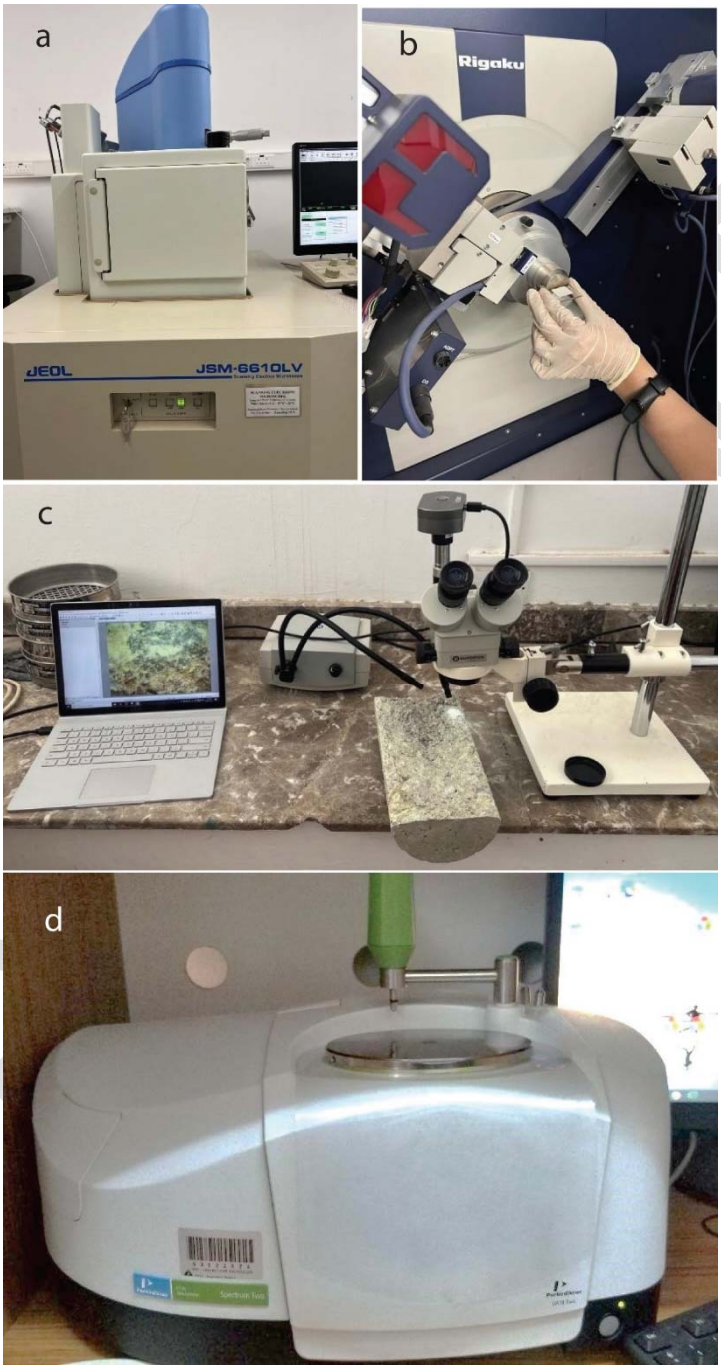

Fig.8 - Equipment used for microstructural analysis: (a): SEM (JEOL JSM-6610LV), (b): XRD (Rigaku), (c): optical microscope, and (d): FTIR spectrometer

2.5.4. Corrosion Test

The corrosion resistance of the concrete specimens was evaluated through an Accelerated Corrosion Test by Impressed Voltage (ACTIV), simulating aggressive chloride environment. A 12V DC voltage was continuously applied while partially immersing the specimens in a 5% NaCl solution. Copper served as the cathode and embedded steel rebars acted as the anode. The electrochemical reactions followed Faraday's laws, where iron oxidizes at the anode ($Fe \rightarrow Fe^{2+} + 2e^-$) and reduction occurs at the cathode ($2H^+ + 2e^- \rightarrow H_2$). The total reaction is represented by: $Fe + 2H^+ \rightarrow Fe^{2+} + H_2$. The corrosion rate (CR) was quantified using Faraday's Second Law:

$$m = \frac{Q.M}{z.F} \tag{3}$$

where m is the mass loss (g), Q is the electric charge (C), M is the molar mass of iron (55.845 g/mol), z is the number of electrons exchanged (2), and F is Faraday's constant (96485 C/mol). To express this as a corrosion rate (mm/year), the ASTM G1-03 [34]formula was used:

$$CR = \frac{K.W}{A.D.T} \tag{4}$$

where $K = 8.76 \times 10^4$, W is the mass loss (g), A is the exposed area of steel (cm^2), D is the steel density (7.85 g/cm^3), and T is the test duration (hours). Crack initiation and progression were monitored visually, and current intensity was recorded daily, enabling comparative evaluation of corrosion behavior across concrete types.

Fig.9 - Setup of accelerated corrosion test using partially immersed specimens and DC power supply.

Fig.9 displays the experimental setup and equipment used for the accelerated corrosion test, illustrating the electrical connections and partially immersed reinforced specimens.

3. RESULTS AND DISCUSSION

3.1. Mechanical Properties

The influence of polymer modifier type and dosage on the mechanical performance of sulfur concrete is illustrated in the three comparative bar charts covering compressive, flexural, and tensile strengths, Fig.10. Overall, the results demonstrate that mechanical properties initially improve with modifier addition up to 5%, followed by a gradual decline as the dosage increases to 20%. For compressive strength, the control mix achieved 20.6 MPa, while the addition of 5% HDPE and LLDPE increased the strength to 23.4 MPa and 25.2 MPa, respectively.

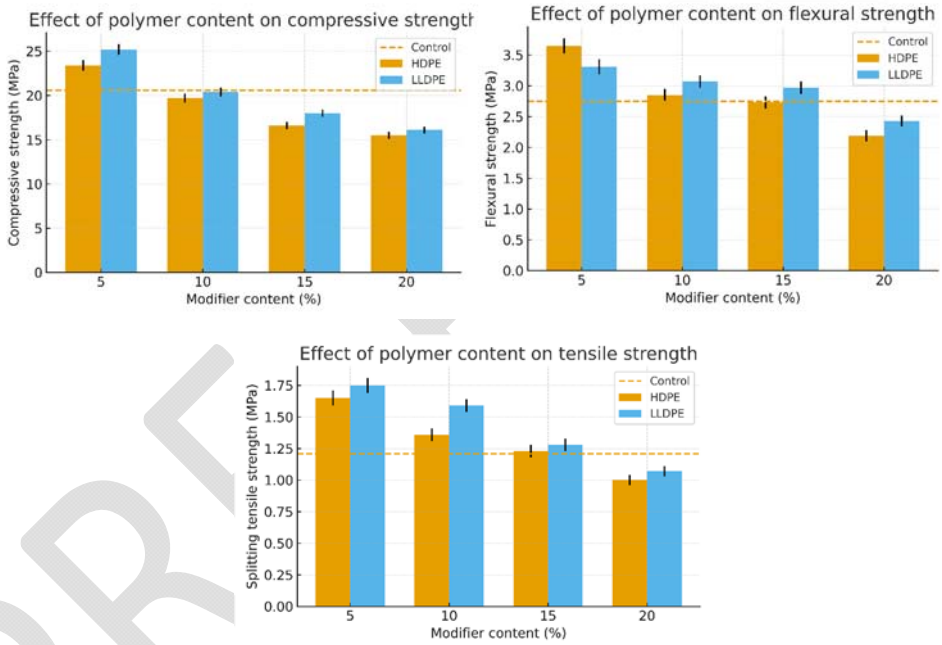

Fig.10 - Effect of HDPE and LLDPE content (5–20 wt.%) on compressive, flexural, and tensile strengths of sulfur concrete.

The mechanical trends observed in this study-an increase of about 14–22% in compressive strength at 5 wt.% HDPE/LLDPE followed by a reduction at higher dosages-are consistent with previous research on sulfur-based composites. Dugarte et al. reported that an additive/sulfur ratio of 0.05–0.10 increased the compressive strength of modified sulfur concrete by roughly 20–30% compared with the reference mix, whereas higher additive contents led to pronounced strength losses [4]. Similar optimum ranges have been noted in

sulfur-modified binders and sulfur-composite systems, where small amounts of technical sulfur or fiber reinforcement improved strength, but further additions caused matrix heterogeneity and strength degradation [35]. Overall, the present results fall within the lower part of the compressive-strength range reported for modified sulfur concretes, but they follow the same characteristic pattern of "optimum modifier content" identified in the literature.

However, beyond 10% dosage, a noticeable decline was observed, with HDPE dropping to 15.5 MPa and LLDPE to 16.1 MPa at 20% dosage. A similar trend was evident in flexural strength: both modifiers enhanced the flexural capacity significantly at 5% (HDPE: 3.65 MPa, LLDPE: 3.31 MPa) compared to the control (2.75 MPa), but the values diminished steadily at higher percentages, with 20% HDPE reaching only 2.19 MPa. In the case of tensile strength, improvements peaked at 5% (HDPE: 1.65 MPa, LLDPE: 1.75 MPa) relative to the control (1.21 MPa), before reducing at higher concentrations (HDPE: 1.00 MPa, LLDPE: 1.07 MPa at 20%). This consistent pattern across all three mechanical tests indicates that low concentrations of polymer modifiers effectively enhance the performance of sulfur concrete, while excessive amounts adversely affect its structural integrity, likely due to poor dispersion or polymer agglomeration within the matrix.

3.2. Ultrasonic Pulse Velocity and Schmidt Hammer Tests

The ultrasonic pulse velocity (UPV) and rebound values were evaluated for sulfur concrete specimens modified with varying proportions (5–20%) of HDPE and LLDPE, as shown in Table 2. The UPV results ranged from 3650 to 4400 m/s for LLDPE and 3650 to 4330 m/s for HDPE. The highest UPV was recorded for LLDPE at 5% (4400 m/s), followed closely by HDPE at 5% (4330 m/s). Similarly, rebound values were higher in LLDPE samples (up to 29.15) than HDPE (maximum 28.1).

Using the SONREB equation, the estimated compressive strength revealed a declining trend with increasing modifier content. For instance, in HDPE-modified samples, the strength decreased from 22.05 MPa at 5% to 14.98 MPa at 20%. A similar reduction was observed in LLDPE samples, albeit with generally higher strength, reaching a peak of 26.14 MPa at 5%.

This trend suggests that while low polymer content improves internal compactness and mechanical performance, excessive modification may lead to a reduction in matrix continuity and bonding, negatively impacting the strength. Thus, 5% LLDPE and HDPE demonstrated optimal performance in terms of both NDT measurements and predicted compressive strength. A comparison of HDPE- and LLDPE-modified specimens at equal dosages shows that LLDPE generally yields slightly higher UPV, rebound values, and estimated compressive strength than HDPE. This behavior can be attributed to differences in polymer chain architecture and their interaction with the sulfur matrix. LLDPE, which contains short-chain branching and has lower crystallinity than HDPE, exhibits greater flexibility and can more effectively penetrate and fill microvoids at the sulfur–aggregate interface at low dosages (5–10 wt.%). This improves stress-wave transmission and dynamic stiffness, leading to higher UPV and rebound readings. HDPE, by contrast, is more crystalline and stiffer, promoting the formation of dense but locally polymer-rich regions, as also suggested by SEM observations, which may introduce additional acoustic impedance

contrasts and slightly reduce the effective pulse velocity. At higher dosages (≥15 wt.%), both polymers tend to agglomerate and increase heterogeneity and porosity, explaining the reduction in UPV and estimated strength for both HDPE- and LLDPE-modified mixes. Nonetheless, the differences between the two modifiers remain modest compared with the overall influence of polymer dosage.

Table 2 - Summary of UPV, rebound values, and estimated compressive strength for sulfur concrete with different HDPE and LLDPE contents (5–20 wt.%).

ID	Modifier (%)	Polymer	UPV (m/s)	Rebound Value (R)	Compressive Strength (MPa)	Experimental Compressive Strength (MPa)
H-5-4	5	HDPE	4330	25.2	22.05	23.4
H-10-4	10	HDPE	4140	22.3	17.5	19.7
H-15-4	15	HDPE	4080	21.3	16.14	16.6
H-20-4	20	HDPE	3650	28.1	14.98	15.5
L-5-4	5	LLDPE	4400	29.15	26.14	25.2
L-10-4	10	LLDPE	4180	27.8	21.73	20.4
L-15-4	15	LLDPE	4070	28.6	20.66	18.0
L-20-4	20	LLDPE	3510	28.55	13.61	16.1

3.3. Microstructural Assessment

The stereomicroscopic image shows well-distributed aggregates within the modified sulfur concrete matrix, as shown in Fig.11. Notable inclusions measured up to 3.44 mm and 3.32 mm, while a void and microcrack were observed at 0.94 mm and 0.26 mm, respectively. These features suggest moderate porosity and potential microcracking, likely due to thermal effects or incomplete bonding. Overall, the compact structure supports the UPV findings, confirming improved internal density at lower polymer contents and aligning with observed mechanical performance trends. Similar microstructural features have been reported in sulfur-based concretes, where increased porosity and microcracking observed by stereomicroscopy/SEM were correlated with lower UPV and compressive strength, while denser matrices showed superior mechanical performance [3,4].

Figs. 12 and 13 present the SEM micrographs of sulfur concrete specimens modified with HDPE and LLDPE, respectively, at varying magnifications, highlighting the influence of polymer type on microstructural development. The HDPE-modified specimens exhibit a relatively dense matrix, with fewer visible voids and smoother fracture surfaces, particularly at higher magnifications (×1000 and ×2000). These features indicate effective polymer dispersion and enhanced interfacial bonding between the polymer phase and the sulfur

matrix. In contrast, the LLDPE-modified specimens exhibit a more heterogeneous microstructure, characterized by increased porosity and poorly bonded regions, as indicated by their irregular surfaces and visible voids. The observed differences in matrix homogeneity and pore distribution align with the mechanical test results, further supporting the improved performance of HDPE-modified mixtures over those containing LLDPE. These microstructural observations confirm that polymer compatibility and dispersion play critical roles in determining the mechanical integrity of modified sulfur concretes.

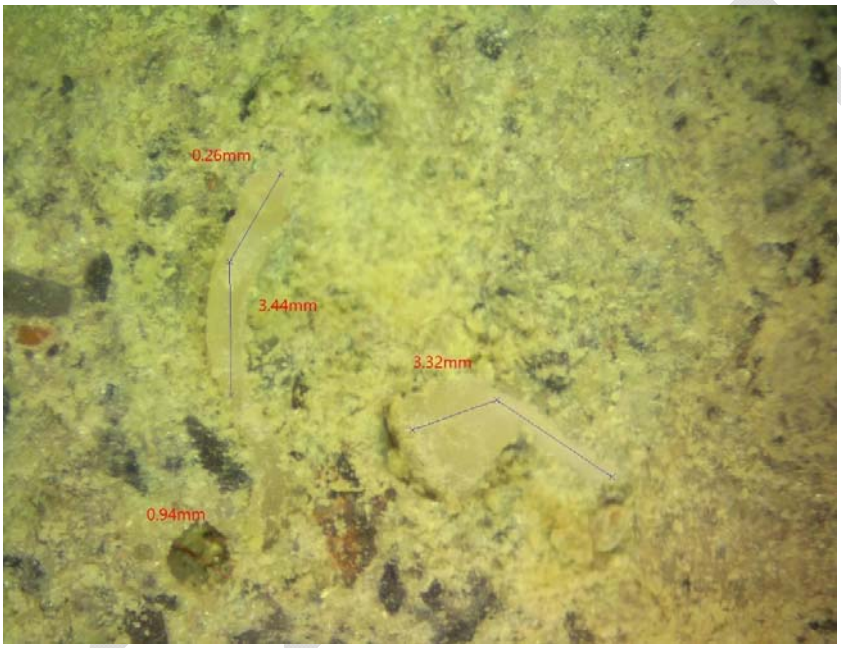

Fig. 11 - Stereomicroscopic view; inclusions, voids, microcracks, and aggregate distribution.

In order to clarify the observed features, the main microstructural constituents have been explicitly labelled in Figs. 12 and 13. In each SEM image, the continuous sulfur matrix is marked as M, unreacted/ recrystallized sulfur or polymer-rich domains as S/P, aggregate particles as Ag, and pores or microcracks as V. These annotations highlight the denser, well-bonded matrix with fewer V regions in the HDPE-modified mixes (Fig. 12), compared with the more porous and heterogeneously bonded structure observed for LLDPE-modified mixes (Fig. 13).

To investigate the chemical stability and potential interactions between sulfur and polymer modifiers, FTIR spectroscopy was conducted prior to mechanical testing. Fig.14 presents the FTIR spectra of sulfur, HDPE, LLDPE, and their respective sulfur-polymer composites (S+HDPE and S+LLDPE). A characteristic absorption band near ~465 cm^{-1}, attributed to the S–S stretching vibration in elemental sulfur (S_8), is evident in all sulfur-containing spectra, confirming the preservation of sulfur's molecular structure during blending. HDPE

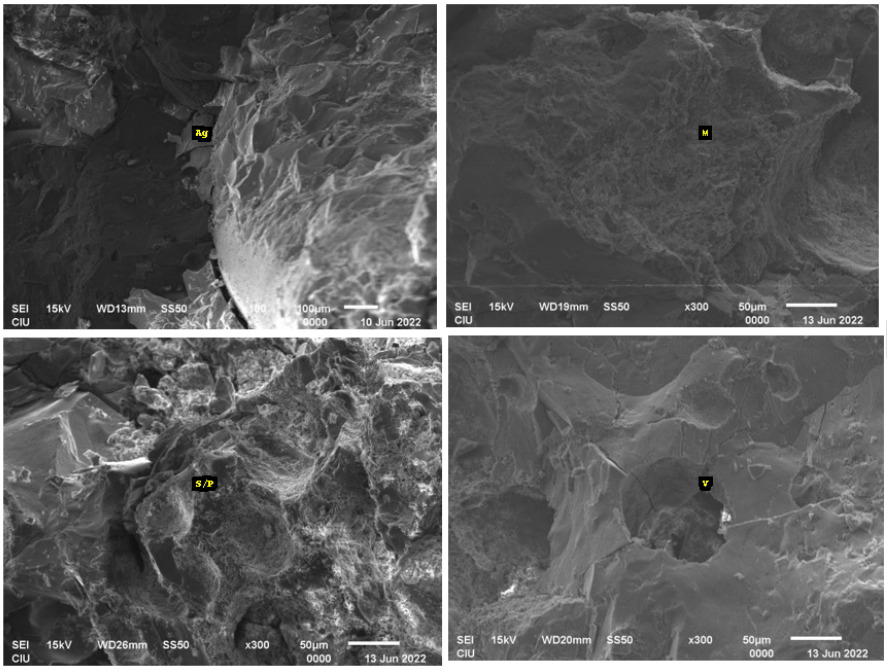

Fig.12 - HDPE-modified sulfur concrete, SEM images at varying magnifications.

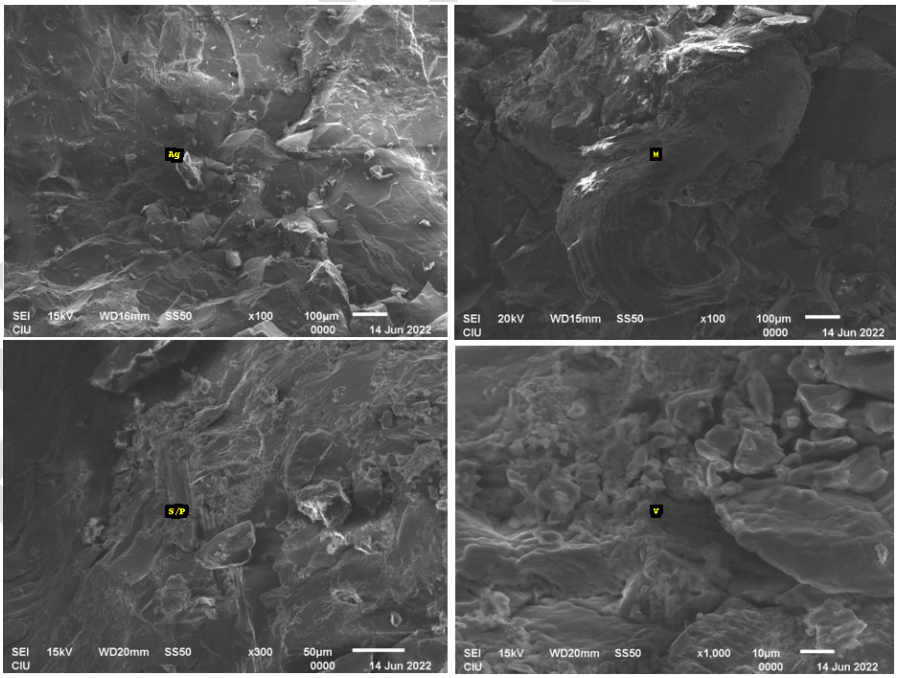

Fig.13 - LLDPE-modified sulfur concrete, SEM images at varying magnifications.

exhibits distinct peaks at ~720 cm^{-1} and ~1460 cm^{-1}, corresponding to methylene rocking and bending vibrations, while the bands in the 1115–1250 cm^{-1} range indicate C–H bond bending. These characteristic peaks are retained in the sulfur-polymer composites, indicating that the polymers remain chemically stable after blending. Crucially, no new peaks were detected in the composite spectra, indicating the absence of chemical reactions or new bond formation between sulfur and the polymers. These observations affirm the physical blending nature of the sulfur-polymer system and are consistent with previous findings in the literature written by Jena and Alhassan [25].

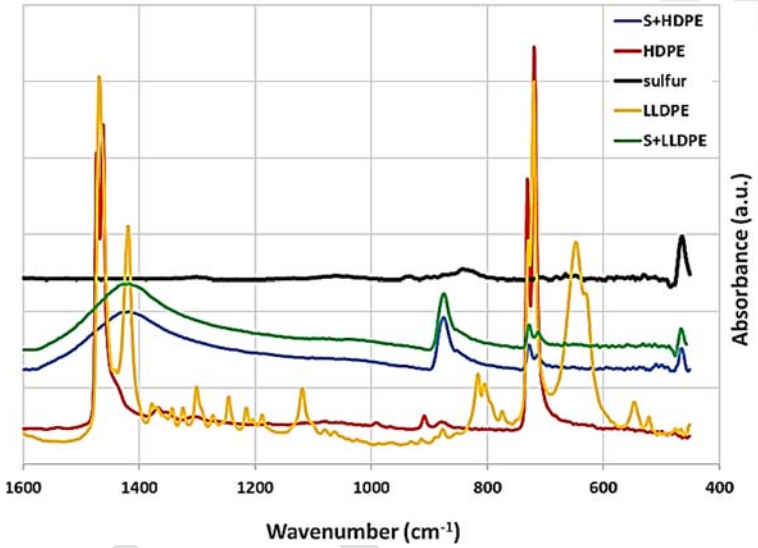

Fig.14 - FTIR spectra of sulfur, polymers (HDPE and LLDPE), and their composites (S+HDPE, S+LLDPE)

The X-ray diffraction (XRD) patterns of sulfur composites modified with 5 wt.% and 20 wt.% of HDPE and LLDPE are presented in Fig.15. All samples exhibited prominent diffraction peaks in the range of $2\theta = 15°–35°$, characteristic of crystalline orthorhombic sulfur (α-S_8). The retention of these peaks across all modified composites suggests that the addition of both HDPE and LLDPE does not alter the fundamental crystalline structure of sulfur. However, minor variations in peak intensity and sharpness were observed, particularly at $2\theta \approx 23.1°$ and 28.6°, which may indicate differences in the degree of crystallinity influenced by the type and content of polymer. The samples containing 20 wt.% of HDPE and LLDPE demonstrated slightly broader and less intense peaks compared to their 5 wt.% counterparts, implying a modest reduction in crystallinity due to the higher polymer loading. These findings suggest that the polymers were physically dispersed within the sulfur matrix without initiating chemical reactions that would disrupt the crystalline phase. Overall, the XRD results confirm the phase stability of sulfur in the presence of HDPE and LLDPE, supporting the formation of structurally integrated but chemically inert sulfur–polymer composites.

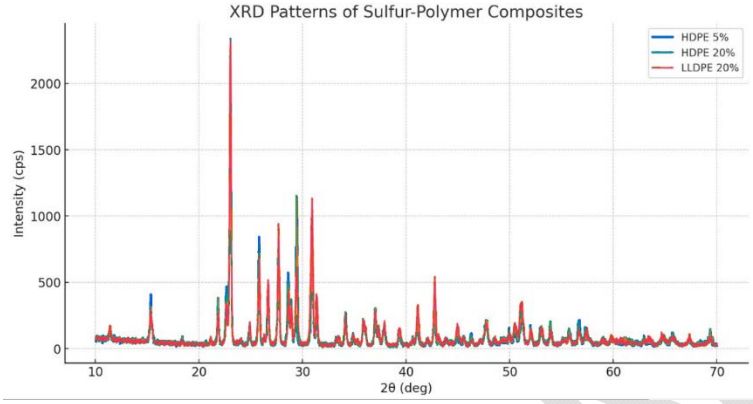

Fig.15 - XRD patterns of sulfur–polymer composites with 5% and 20% HDPE/LLDPE showing preserved α-S_8 crystalline peaks.

3.4. Corrosion Assessment

The corrosion behavior of the modified sulfur concrete mixes was evaluated using an impressed voltage technique over a 14-day period, and the recorded current values are illustrated in Fig.16. The unmodified sulfur concrete (Control) exhibited the highest current intensity throughout the testing period, indicating greater electrochemical activity and, consequently, a higher corrosion rate of the embedded steel. This behavior can be attributed to the relatively higher permeability and lack of polymer-induced barrier effects in the control mix.

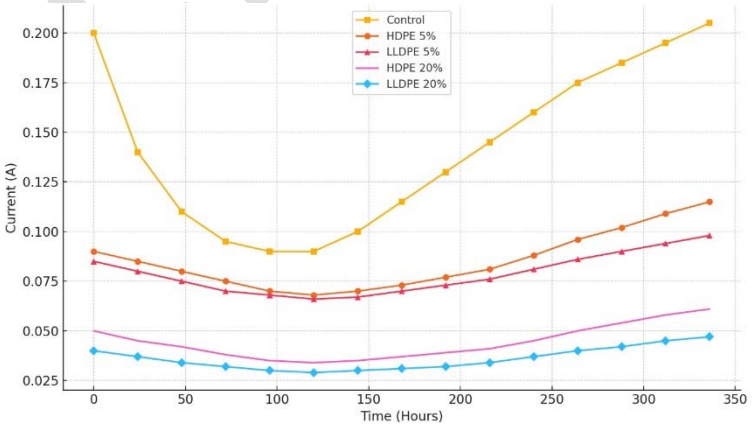

Fig.16 - Current–time response of sulfur concrete with different HDPE and LLDPE contents under impressed voltage over 14 days.

In contrast, all polymer-modified mixes demonstrated significantly improved corrosion resistance. Notably, the mixes incorporating 20% HDPE and 20% LLDPE exhibited the lowest current values, indicative of a more stable passive layer on the rebar surface and effective inhibition of ionic migration through the concrete matrix. This enhanced resistance is attributed to the hydrophobic nature and crack-bridging capacity of the polymers, which likely reduced the ingress of chloride ions and moisture. The 5% HDPE and 5% LLDPE mixes also performed better than the control group, but with moderately higher current levels compared to their 20% counterparts, suggesting a dose-dependent effectiveness of polymer modification. This enhanced resistance is attributed to the hydrophobic and electrically insulating nature of the polymer phase and to its ability, after softening during hot mixing, to form ductile films and ligaments that blunt and partially bridge microcracks, thereby reducing crack width and the connectivity of transport paths for chloride ions and moisture.

4. CONCLUSION

This study investigated the mechanical properties, microstructural characteristics, and corrosion resistance of sulfur concrete modified with HDPE and LLDPE. A novel temperature-controlled laboratory mixer was employed to achieve homogeneous mixing conditions. The key findings provide practical insights for optimizing polymer-modified sulfur concrete for sustainable construction applications:

i. Optimal mechanical performance at 5 wt.% polymer dosage: Incorporation of 5 wt.% HDPE and LLDPE notably enhanced mechanical properties, with maximum compressive strength increasing by 22.5% (from 20.6 MPa to 25.24 MPa). Flexural and tensile strengths also peaked at 5 wt.% polymer content, reaching 3.65 MPa and 1.75 MPa respectively. Higher polymer dosages (15–20 wt.%) caused performance degradation due to polymer agglomeration and reduced matrix integrity.

ii. Enhanced compactness verified by non-destructive testing:

    The highest ultrasonic pulse velocity (4400 m/s) and rebound hammer value (29.15) were obtained with 5 wt.% LLDPE, correlating well with the highest estimated compressive strength (26.14 MPa). These non-destructive test outcomes confirm improved internal density and optimal compactness at lower polymer content.

iii. Microstructural analyses validated physical reinforcement mechanisms: SEM analysis revealed denser and more homogenous microstructure in HDPE modified specimens, whereas LLDPE-modified samples exhibited greater porosity. FTIR confirmed the absence of new chemical bonds, while XRD showed the retention of α-S_8 crystalline structures across all samples, with slight reductions in crystallinity at higher polymer loadings, affirming a purely physical blending mechanism.

iv. Dose-dependent improvement in corrosion resistance:

    Accelerated corrosion testing demonstrated significant improvements in corrosion resistance with increasing polymer content, where 20 wt.% HDPE and LLDPE showed the lowest current intensities (~0.03 A), indicating effective reduction in chloride permeability and improved barrier performance. Even at the lowest dosage (5 wt.%),

polymer modification outperformed the control group, underscoring the protective benefits of polymer integration.

v. The optimized sulfur–polymer concretes, with compressive strengths of about 20–25 MPa and rapid setting, are suitable for industrial floors, precast blocks, drainage elements, and pavement overlays in aggressive environments.

vi. Sulfur is an inexpensive by-product and the optimum polymer content is low (≈5 wt.%), so the extra material cost is modest and can be offset by faster construction and the elimination of water curing.

These findings underscore the necessity of optimized polymer dosage in sulfur concrete to balance mechanical performance, structural integrity, and corrosion resistance, offering guidance for practical, durable, and sustainable infrastructure solutions. Although the present investigation was carried out at laboratory scale, the findings provide a technical basis for future professional applications of polymer-modified sulfur concrete. Follow-up studies will focus on (i) scaling up the temperature-controlled mixer for semi-industrial production, (ii) pilot implementation in precast elements and pavement blocks under realistic service conditions, (iii) extended durability assessments (e.g., freeze–thaw, thermal and moisture cycling, abrasion, and long-term corrosion performance), and (iv) development of mix-design and quality-control guidelines to facilitate safe and reliable adoption in engineering practice.

References

[1] R.M. Andrew, Global CO2 emissions from cement production, 1928-2018, Earth Syst Sci Data 11 (2019) 1675–1710. https://doi.org/10.5194/ESSD-11-1675-2019.

[2] R. Fediuk, Y.H. Mugahed Amran, M.A. Mosaberpanah, A. Danish, M. El-Zeadani, S. V. Klyuev, N. Vatin, A critical review on the properties and applications of sulfur-based concrete, Materials 13 (2020). https://doi.org/10.3390/ma13214712.

[3] A.-M.Onsy. Mohamed, M. El-Gamal, Sulfur concrete for the construction industry : a sustainable development approach, J. Ross Pub, 2010.

[4] M. Dugarte, G. Martinez-Arguelles, J. Torres, Experimental evaluation of modified sulfur concrete for achieving sustainability in industry applications, Sustainability (Switzerland) 11 (2018). https://doi.org/10.3390/su11010070.

[5] N. Amanova, K. Turaev, M.H. Shadhar, U. Tadjixodjayeva, Z. Jumaeva, E. Berdimurodov, I. Eliboev, A. Hosseini-Bandegharaei, Sulfur-based concrete: Modifications, advancements, and future prospects, Constr Build Mater 435 (2024) 136765. https://doi.org/10.1016/J.CONBUILDMAT.2024.136765.

[6] S.A. Stel'makh, E.M. Shcherban', A.N. Beskopylny, L.R. Mailyan, B. Meskhi, A.A. Shilov, A. Evtushenko, A. Chernil'nik, D. El'shaeva, M. Karalar, Y.O. Özkılıç, C. Aksoylu, Physical, Mechanical and Structural Characteristics of Sulfur Concrete with Bitumen Modified Sulfur and Fly Ash, Journal of Composites Science 7 (2023). https://doi.org/10.3390/jcs7090356.

[7] J. Moon, P.D. Kalb, L. Milian, P.A. Northrup, Characterization of a sustainable sulfur polymer concrete using activated fillers, Cem Concr Compos 67 (2016) 20–29. https://doi.org/10.1016/J.CEMCONCOMP.2015.12.002.

[8] S. Ghasemi, M.R. Nikudel, A. Zalooli, M. Khamehchiyan, A. Alizadeh, F. Yousefvand, A.M.R. Ghasemi, Durability Assessment of Sulfur Concrete and Portland Concrete in Laboratory Conditions and Marine Environments, Journal of Materials in Civil Engineering 34 (2022) 04022167. https://doi.org/10.1061/(ASCE)MT.1943-5533.0004320.

[9] M.M. El Gamal, A.S. El-Dieb, A.M.O. Mohamed, K.M. El Sawy, Performance of modified sulfur concrete exposed to actual sewerage environment with variable temperature, humidity and gases, Journal of Building Engineering 11 (2017). https://doi.org/10.1016/j.jobe.2017.03.009.

[10] B. Łaźniewska-Piekarczyk, Research on the Possibilities of Using Sulfur Concrete for Road Infrastructure Construction—Assessment Based on European Standards, Sustainability (Switzerland) 17 (2025). https://doi.org/10.3390/SU17083671.

[11] O. Öztürk, A. Öner, Long-term Durability of Bitumen Modified Sulfur Polymer Concrete Under Freeze–Thaw Cycles, International Journal of Civil Engineering 2021 20:5 20 (2021) 529–543. https://doi.org/10.1007/S40999-021-00672-2.

[12] M.A. Gulzar, A. Rahim, B. Ali, A.H. Khan, An investigation on recycling potential of sulfur concrete, Journal of Building Engineering 38 (2021). https://doi.org/10.1016/j.jobe.2021.102175.

[13] J. Liu, J. Zhang, C. Yan, S. Liu, Z. Jiang, Bonding Performance of Sulfur-Based Polymers for Pavement Repair, Journal of Transportation Engineering, Part B: Pavements 149 (2023) 04023031. https://doi.org/10.1061/JPEODX.PVENG-1164;PAGEGROUP:STRING:PUBLICATION.

[14] J. Liu, C. Yan, J. Li, J. Zhang, S. Liu, Investigation on the Mechanical Properties and Strengthening Mechanism of Solid-Waste–Sulfur-Based Cementitious Composites, Materials 2023, Vol. 16, Page 1203 16 (2023) 1203. https://doi.org/10.3390/MA16031203.

[15] X. You, X. You, Research Progress of the Modification in Sulfur Concrete, Materials Sciences and Applications 12 (2021) 353–361. https://doi.org/10.4236/MSA.2021.127024.

[16] M. Mann, B. Zhang, S. Tonkin, C. Gibson, Z. Jia, T. Hasell, J. Chalker, Process for coating surfaces with a copolymer made from sulfur and dicyclopentadiene, (2021). https://doi.org/10.33774/CHEMRXIV-2021-N91H4.

[17] M. Porto, P. Caputo, V. Loise, S. Eskandarsefat, B. Teltayev, C.O. Rossi, Bitumen and bitumen modification: A review on latest advances, Applied Sciences (Switzerland) 9 (2019) 742. https://doi.org/10.3390/app9040742.

[18] S. Abeysinghe, C. Gunasekara, C. Bandara, K. Nguyen, R. Dissanayake, P. Mendis, Engineering Performance of Concrete Incorporated with Recycled High-Density Polyethylene (HDPE)—A Systematic Review, Polymers 2021, Vol. 13, Page 1885 13 (2021) 1885. https://doi.org/10.3390/POLYM13111885.

[19] T. Wani, S.A.Q. Pasha, S. Poddar, B.H. V, A Review on the use of High Density Polyethylene (HDPE) in Concrete Mixture, International Journal of Engineering Research & Technology 9 (2020). https://doi.org/10.17577/IJERTV9IS050569.

[20] Y. Aocharoen, P. Chotickai, Compressive mechanical and durability properties of concrete with polyethylene terephthalate and high-density polyethylene aggregates, Clean Eng Technol 12 (2023) 100600. https://doi.org/10.1016/J.CLET.2023.100600.

[21] M.H. Shahsavari, M.M. Karbala, S. Iranfar, V. Vandeginste, Martian and lunar sulfur concrete mechanical and chemical properties considering regolith ingredients and sublimation, Constr Build Mater 350 (2022) 128914. https://doi.org/10.1016/J.CONBUILDMAT.2022.128914.

[22] ASTM C33/C33M ASTM International, Standard Specification for Concrete Aggregates, West Conshohocken, PA, 2018.

[23] J. Liu, C. Yan, J. Zhang, S. Liu, P. Li, Experimental study and modeling analysis of strength properties of sulfur-based polymers of waste ceramic fine aggregates, Mater Chem Phys 301 (2023) 127614. https://doi.org/10.1016/J.MATCHEMPHYS.2023.127614.

[24] B. Wang, J. Zhang, C. Yan, J. Li, P. Li, Mechanical Properties and Microstructure of Sulfur Polymer Composite Containing Basalt Fibers, KSCE Journal of Civil Engineering 26 (2022) 5199–5209. https://doi.org/10.1007/s12205-022-0006-8.

[25] K.K. Jena, S.M. Alhassan, Melt processed elemental sulfur reinforced polyethylene composites, J. Appl. Polym. Sci (2015) 43060. https://doi.org/10.1002/app.43060.

[26] R. Anyszka, D. Bielinski, M. Imiela, P. Szajerski, J. Pawlica, R. Walendziak, M. Sicinski, Sulfur Concrete – Promising Material for Space-Structures Building, in: in Proceedings of the European conference on spacecraft structures materials and environmental testing, Toulouse, France, 2016.

[27] British Standards Institution, BS EN 12390-3:2009 – Testing hardened concrete – Part 3: Compressive strength of test specimens, London, UK, 2009.

[28] British Standards Institution (BSI), BS EN 12390-6:2009 Testing hardened concrete — Part 6: Tensile splitting strength of test specimens, 2009.

[29] ASTM C78/C78M-18 ASTM International, Standard Test Method for Flexural Strength of Concrete (Using Simple Beam with Third-Point Loading), West Conshohocken, PA, 2018.

[30] British Standards Institution (BSI), BS EN 12504 2:2021 Testing concrete in structures – Part 2: Non destructive testing – Determination of rebound number, 2021.

[31] ASTM C805/C805M 18 ASTM International, Standard Test Method for Rebound Number of Hardened Concrete, West Conshohocken, PA, 2018.

[32] A. Ndagi, A.A. Umar, F. Hejazi, M.S. Jaafar, Non-destructive assessment of concrete deterioration by ultrasonic pulse velocity: A review, IOP Conf Ser Earth Environ Sci 357 (2019). https://doi.org/10.1088/1755-1315/357/1/012015.

[33] N.R. Chandak, H.R. Kumavat, SonReb Method for Evaluation of Compressive Strength of Concrete, IOP Conf Ser Mater Sci Eng 810 (2020). https://doi.org/10.1088/1757-899X/810/1/012071.

[34] ASTM G1 03 ASTM International, Standard Practice for Preparing, Cleaning, and Evaluating Corrosion Test Specimens, West Conshohocken, PA, 2003.

[35] S.A. Stel'makh, E.M. Shcherban', A.N. Beskopylny, L.R. Mailyan, A.A. Shilov, I. Razveeva, S. Oganesyan, A. Pogrebnyak, A. Chernil'nik, D. Elshaeva, Enhancing the Mechanical Properties of Sulfur-Modified Fly Ash/Metakaolin Geopolymers with Polypropylene Fibers, Polymers 2025, Vol. 17, Page 2119 17 (2025) 2119. https://doi.org/10.3390/POLYM17152119.